

SparseMap: Loop Mapping for Sparse CNNs on Streaming Coarse-grained Reconfigurable Array

XIAOBING NI, School of Microelectronics, University of Science and Technology of China, China
 MENGKE GE, Institute of Artificial Intelligence, Hefei Comprehensive National Science Center, China
 and School of Microelectronics, University of Science and Technology of China, China
 JIAHENG RUAN, School of Microelectronics, University of Science and Technology of China, China
 SONG CHEN, YI KANG, School of Microelectronics, University of Science and Technology of China,
 China and Institute of Artificial Intelligence, Hefei Comprehensive National Science Center, China

Streaming coarse-grained reconfigurable array (CGRA) is a promising architecture for data/computing-intensive applications because of its flexibility, high throughput and efficient memory system. However, when accelerating sparse CNNs, the irregular input data demands inside sparse CNNs would cause excessive caching operations (COPs) and multi-cycle internal dependencies (MCIDs) between operations, declining the throughput of the streaming CGRA. We propose a mapping method for sparse CNNs onto streaming CGRA, SparseMap, which incorporates an efficient I/O data management along with operation scheduling and binding, to reduce the COPs and MCIDs, thereby ensuring the optimal throughput of streaming CGRA. The experimental results show SparseMap reduces 92.5% COPs and 46.0 % MCIDs while achieves the same or even smaller initiation interval (II) compared to previous works.

CCS Concepts: • **Computer systems organization** → **Reconfigurable computing**; • **Computing methodologies** → *Parallel computing methodologies*; • **Theory of computation** → Models of computation.

Additional Key Words and Phrases: Streaming CGRA, sparse CNNs, irregular input demands, COPs, MCIDs, SparseMap, I/O data management.

ACM Reference Format:

Xiaobing Ni, Mengke Ge, Jiaheng Ruan, and Song Chen, Yi Kang. 2024. SparseMap: Loop Mapping for Sparse CNNs on Streaming Coarse-grained Reconfigurable Array. *J. ACM* 37, 4, Article 111 (August 2024), 12 pages. <https://doi.org/XXXXXXXX.XXXXXXX>

This work was supported in part by the Strategic Priority Research Program of Chinese Academy of Sciences, Grant No. XDB44000000, in part by the University Synergy Innovation Program of Anhui Province under grant No. GXXT-2023-003, and in part by CAS Project for Young Scientists in Basic Research under grant No. YSBR-029. (*Corresponding author: Song Chen*).

Authors' addresses: Xiaobing Ni, nxb@mail.ustc.edu.cn, School of Microelectronics, University of Science and Technology of China, Hefei, Anhui, China; Mengke Ge, mengke.ge@iai.ustc.edu.cn, Institute of Artificial Intelligence, Hefei Comprehensive National Science Center, Hefei, Anhui, China and School of Microelectronics, University of Science and Technology of China, Hefei, Anhui, China; Jiaheng Ruan, handso@mail.ustc.edu.cn, School of Microelectronics, University of Science and Technology of China, Hefei, Anhui, China; Song Chen, Yi Kang, songch,ykang@ustc.edu.cn, School of Microelectronics, University of Science and Technology of China, Hefei, Anhui, China and Institute of Artificial Intelligence, Hefei Comprehensive National Science Center, Hefei, Anhui, China.

Permission to make digital or hard copies of all or part of this work for personal or classroom use is granted without fee provided that copies are not made or distributed for profit or commercial advantage and that copies bear this notice and the full citation on the first page. Copyrights for components of this work owned by others than the author(s) must be honored. Abstracting with credit is permitted. To copy otherwise, or republish, to post on servers or to redistribute to lists, requires prior specific permission and/or a fee. Request permissions from permissions@acm.org.

© 2024 Copyright held by the owner/author(s). Publication rights licensed to ACM.

0004-5411/2024/8-ART111 \$15.00

<https://doi.org/XXXXXXXX.XXXXXXX>

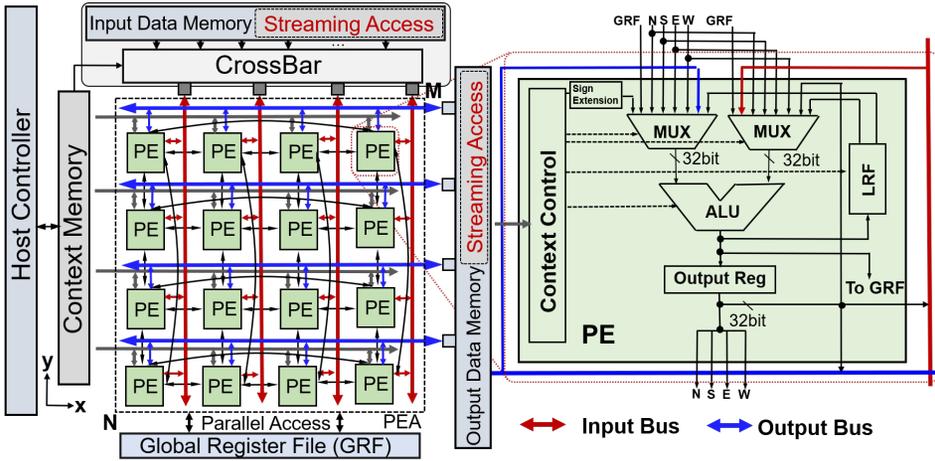


Fig. 1. Streaming CGRA.

1 INTRODUCTION

CGRA, combining energy efficiency and flexibility, is a promising architecture for data/computing-intensive applications[1–4]. Inspired by the streaming access property inherent to data/computing-intensive applications, a streaming CGRA was proposed [1], where on-chip data memories provide a streaming dataflow for the PE array (PEA), avoiding the fragmented and scattered memory access from PEs. In comparison to the common CGRAs utilizing load/store addressing in PEs, the streaming CGRA is more conducive to applications that employ continuous memory addressing, such as CNNs. The streaming CGRA in Fig. 1 is equipped with a PEA, a global register file (GRF), data memories (supporting streaming access), a crossbar and I/O buses.

The CGRA accelerates the applications' kernel loops. The CGRA compiler performs soft pipelining for the loop, schedules loop operations, and binds the operations and internal dependencies to PEs and routing resources[5]. Previous compilers can be categorized into graph based[5–11], cost function based [12–15] and learning based[16][17] methods. These works aimed to minimize the II between adjacent iterations of the loop to maximize the throughput of CGRA. They focused on accelerating the applications on common CGRAs. However, due to the absence of load/store addressing in PEs and no buffer in I/O buses, the compiler for streaming CGRA needs to explicitly manage the I/O data at the PEA side, i.e. allocating I/O data with the correct I/O buses at the appropriate time and caching the I/O data in the PEA if needed, thus ensuring the legal I/O data routing.

CNNs outperform humans [18][19] but with surging computation and memory requirements[20]. Fortunately, the intrinsic sparsity in CNNs significantly lowers these requirements in sparse CNNs[21][22]. The sparse CNN is typically partitioned into multiple sparse blocks which are handled in a predetermined order. Each block computes different channels from different kernels and is abstracted as a sparse data flow graph (*s-DFG*). The non-uniform distribution of non-zero weights and the skipping of zero-weight multiplications would incur irregular input data demands inside *s-DFGs*. The irregularity complicates the management of input data at the PEA side, and further affects the efficiency of the streaming CGRA. Firstly, due to no buffer in I/O buses, PEs would be occupied to cache the input data whose allocating time is inconsistent with the scheduling times of its multiplications. Secondly, without proper bus allocation for input data, the excessive MCIDs between operations would be generated. Limited by the PEA and buffer resources, the

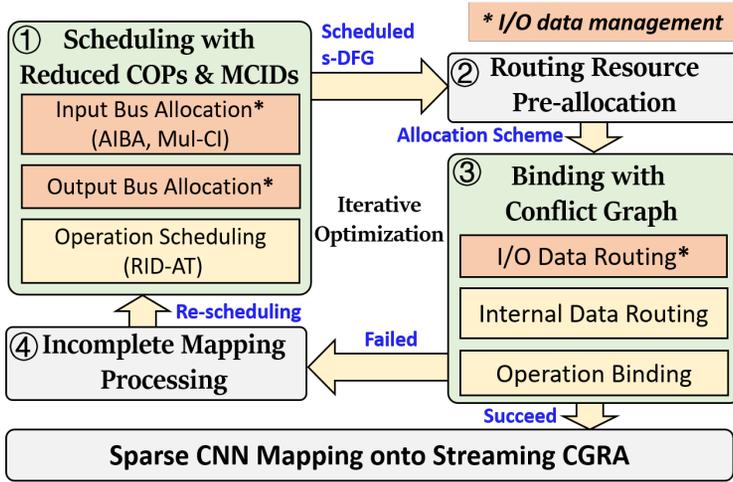


Fig. 2. SparseMap overview.

excessive PEs for caching (corresponding to the COPs inserted into s-DFG) and MCIDs routing may increase the II, thereby declining streaming CGRA's throughput.

In order to address the issue of excessive COPs and MCIDs resulting from the irregular input data demands, we propose SparseMap, a mapping algorithm designed for sparse CNNs in the context of streaming CGRAs. SparseMap employs an efficient I/O data management, along with operation scheduling and binding, to ensure the optimal throughput of streaming CGRAs. It contains contributions as follows:

- To address the challenges posed by the irregular input data demands inside the s-DFG, we present a scheduling approach that not only allocates input buses in accordance with input data demands but also reconstructs the internal dependencies within the adder trees. This enables the s-DFG to be scheduled in a manner that reduces both COPs and MCIDs.
- Given the scheduled s-DFG and streaming CGRA, we propose to construct a conflict graph to represent the binding problem, such that legal operation binding, and I/O data and internal data routing are obtained by solving the maximum independent set (*MIS*) on the graph.
- Compared to previous works, SparseMap achieves fewer COPs and MCIDs while having the same or even smaller II.

The rest of this paper is organized as follows: Section 2 elaborates the way to reduce COPs and MCIDs. Section 3 gives the problem formulation. Section 4 details SparseMap. Section 5 presents experimental results, followed by the conclusion in Section 6.

2 REDUCING COPS AND MCIDS

To reduce the COPs and MCIDs caused by the irregular input data demands, we allocate the input buses considering the demands among multiple input data and within single input data. Moreover, the internal dependencies within the adder trees are to be reconstructed to further reduce the MCIDs.

2.1 Association-Oriented Input Bus Allocation

Any two input data with a high **association** (defined as the number of kernels requiring these two data simultaneously) allocated with input buses at different times would incur excessive MCIDs.

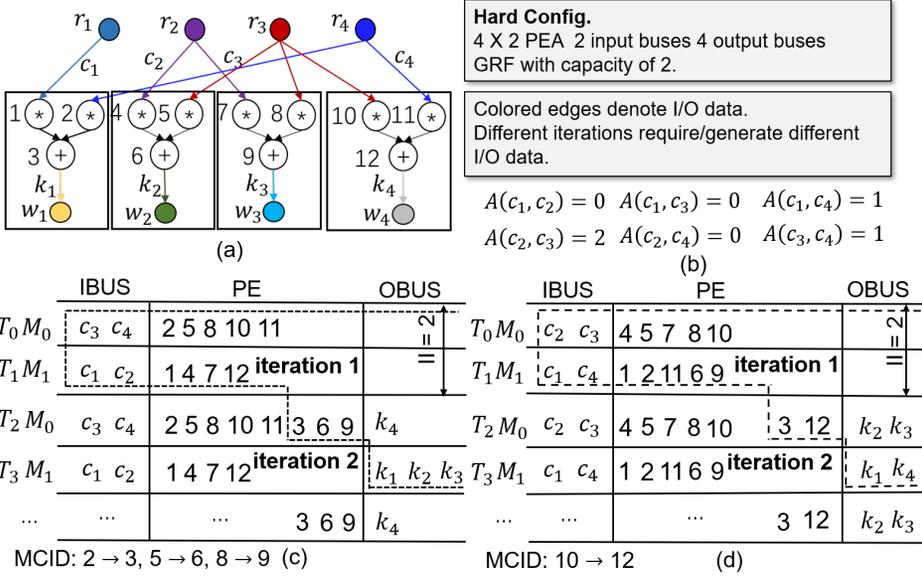


Fig. 3. (a) A s-DFG computing 4 channels from 4 kernels; (b) Input associations; (c) A scheduling with 3 MCIDs; (d) A scheduling with 1 MCID.

Firstly, to avoid the caching PEs, for any input data, the scheduling times of its multiplications should keep same as the allocating time of that data. Secondly, for any addition, at least 1 MCID is generated if its two producers (multiplications or additions) are scheduled at different times. Hence, any two highly associated input data with different allocating times would incur their respective multiplications to be scheduled differently, thereby causing the excessive MCIDs.

We propose an association-oriented input bus allocation (AIBA) method which prioritizes allocating input buses for highly associated input data at the same time, making more multiplications be scheduled together across different kernels, thus reducing the MCIDs. The efficiency of AIBA can be proven in Fig. 3 where the input data c_2 and c_3 with a highest association are allocated with input buses at the same time in Fig. 3(d), reducing the MCIDs from 3 in Fig. 3(c) to 1. Routing via local register file (LRF) for any MCID in Fig. 3(c)-(d) is forbidden due to the same modulo time for the consumer and producer in each MCID[6]. Routing via GRF can be adopted, but is able for 1 MCID at most, causing a failed mapping at $\Pi = 2$ for Fig. 3(c), but a successful mapping for Fig. 3(d). The reduced MCIDs alleviate the routing pressures and ensure the streaming CGRA's throughput.

2.2 Multi-casting Input Data via Crossbar

For the input data with multiplications exceeding the fan-out PEs of an input bus, not all the PEs executing the multiplications can obtain the input data from one input bus directly (the weights are pre-loaded into PEs' LRF). In this case, not all the multiplications can be scheduled at the allocating time of the input data. As Fig. 4(a)-(b) show, on a 4×4 PE, the input data c_0 cannot be directly transferred to 5 PEs executing its multiplications via one input bus, and a COP is required for c_0 . Aided by the multi-casting ability of the crossbar, we propose to multi-cast the input data (Mul-CI) to more input buses (if available) as depicted in Fig. 4(c)-(d), which avoids the COPs and enables more multiplications to be scheduled with the input data. The Mul-CI technique also indirectly guarantees the effectiveness of the AIBA technique.

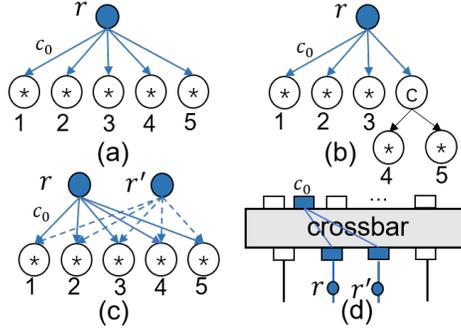


Fig. 4. (a) The input data c_0 with 5 multiplications exceeding fan-out PEs on an input bus in a 4×4 PEA; (b) A COP c inserted into s -DFG; (c) (d) Multi-casting c_0 to 2 input buses by crossbar.

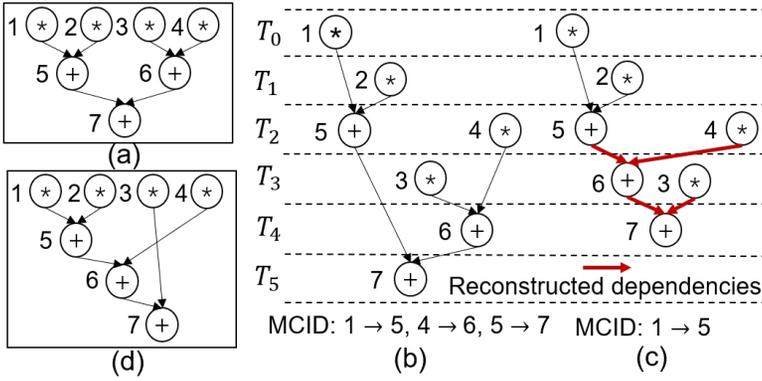


Fig. 5. (a) A kernel with 4 multiplications and 1 adder tree composed by 3 additions; (b) A scheduling with 3 MCIDs for the fixed adder tree. (c) A scheduling with 1 MCID for the reconstructed adder tree; (d) The final kernel after reconstructing the internal dependencies within the adder tree.

2.3 Reconstructing Internal Dependencies within Adder Trees

For a kernel with n multiplications, $n - 1$ additions form an adder tree to accumulate the multiplications. As long as it is guaranteed that there are two producers and one consumer for each addition (except for the last addition), the final accumulated result is unique and correct regardless of the internal dependencies within the adder tree. Based on the observation above, we propose to reconstruct the internal dependencies within the adder tree (**RID-AT**) according to the multiplications' scheduling to further reduce the MCIDs. Section IV details the RID-AT technique. After employing RID-AT for the kernel in Fig. 5(a), the MCIDs in Fig. 5(c) are reduced from 3 to 1 compared with the fixed adder tree in Fig. 5(b).

3 PROBLEM FORMULATION

3.1 Definitions and Notations

The mapping of s -DFG onto streaming CGRA can be decomposed into scheduling and binding[5][6]. Targeting the reduction of COPs and MCIDs, the scheduling determines the scheduling and modulo scheduling times of operations and the I/O bus allocation for the I/O data, subject to the constraints

Table 1. Symbols and descriptions

N, M	$N \times M$ PEA with M input buses, N output buses.
$t(v), m(v)$	The scheduling and modulo scheduling times for $v \in V_D$.
c_r	0-1 variable. c_r is 1 if $r \in V_R$ is cached by a COP.
mc_r	0-1 variable. mc_r is 1 if $r \in V_R$ is multi-cast by crossbar.
$MCID$	$\{(v_1, v_2) \mid (v_1, v_2) \in E_I, t(v_1) - t(v_2) > 1\}$, denoting the set of MCIDs.
$\mathcal{M}_R(i)$	$\{r \mid r \in V_R, m(r) = i\}$, composed of the $r \in V_R$ modulo scheduled at i .
$\mathcal{M}_W(i)$	$\{w \mid w \in V_W, m(w) = i\}$, composed of the $w \in V_W$ modulo scheduled at i .
$\mathcal{M}_{OP}(i)$	$\{op \mid op \in V_{OP}, m(op) = i\}$, composed of the $op \in V_{OP}$ modulo scheduled at i .
$\mathcal{M}_C(i)$	$\{r \mid c_r = 1, m(r) = i\}$, composed of the $r \in V_R$ which is cached by a COP.
$\mathcal{M}_{MC}(i)$	$\{r \mid mc_r = 1, m(r) = i\}$, composed of the $r \in V_R$ which is multi-cast by crossbar.

dependencies, PEA and I/O buses. The binding decides the physical resource required for each node in s-DFG and ensures the legal routing of I/O data and internal data. To clearly define the s-DFG mapping onto streaming CGRA, we introduce I/O reading/writing nodes into s-DFG to facilitate the I/O data management, along with operation scheduling and binding.

(1) *Sparse Data Flow Graph (s-DFG)*: s-DFG is the loop body of the sparse block, denoted as $D = (V_D, E_D)$. V_D is a set composed of multiplications, additions and I/O reading/writing which constitute V_M, V_A, V_R and V_W respectively, and we denote an operation set $V_{OP} = V_M \cup V_A$. Differing from the nodes in V_{OP} executed by PEs, the nodes in V_R (V_W) are operated on input (output) buses, denoting the input (output) data is read from (written to) input (output) buses. E_D is a dependency set containing input dependencies, output dependencies, and internal dependencies, denoted as $E_D = E_R \cup E_W \cup E_I$: $\forall (v_1, v_2) \in E_D$, if $v_1 \in V_R, v_2 \in V_{OP}$, then $(v_1, v_2) \in E_R$; if $v_1 \in V_{OP}, v_2 \in V_W$, then $(v_1, v_2) \in E_W$; otherwise, $(v_1, v_2) \in E_I$. The internal dependencies within the adder trees would be reconstructed in the scheduling phase.

(2) *Initiation Interval (II)*: II is the time slots between adjacent iterations of the loop. The compiler pursues to minimize II to maximize the throughput of the streaming CGRA. After scheduling, $\forall v \in V_D$ is assigned a scheduling time and a modulo scheduling time from 0 to II-1. The (modulo) scheduling time of r ($w \in V_R$ (V_W)) denotes the (modulo) allocating time of the I/O data.

(3) *I/O data management*: The management of I/O data at PEA side can be transformed into the scheduling, caching and binding for the nodes in V_R and V_W . Due to no buffer in I/O buses, the scheduling distance between the consumer and producer of any input (output) dependency can only be 0 (1).

(4) *Time-Extended CGRA (TEC)*: TEC $T = (V_T, E_T, II)$ is a resource graph replicating streaming CGRA from 0 to II-1. V_T is a set composed of replicated resource nodes (including PEs, I/O buses etc.). $\forall v^m \in V_T$ denotes the resource node v located at m -th time layer of the TEC. E_T is a directed edge set. For $v_1^{m_1}, v_2^{m_2} \in V_T$, $v_1^{m_1}$ connects to $v_2^{m_2}$ if and only if $(v_1^{m_1}, v_2^{m_2}) \in E_T, m_2 = m_1 + 1, 0 \leq m_1 < II - 1$, or $m_2 = 0, m_1 = II - 1$ [5][6].

(5) *Conflict Graph (CG) and MIS*: CG $CG = (V_{CG}, E_{CG})$ is a graph reflecting the conflict relations among bindings. V_{CG} contains: tuples $(r^m, ibus_i^m)$, $(w^m, obus_j^m)$ and quadruples $(pe_{i,j}^m, op^m, bus_x^m, bus_y^m)$. $(r^m, ibus_i^m)$ denotes the input reading $r \in V_R$ modulo scheduled at m is allocated with i -th input bus at the m -th time layer of the TEC, so as $(w^m, obus_j^m)$ dose. $(pe_{i,j}^m, op^m, bus_x^m, bus_y^m)$ denotes $op \in V_{OP}$ modulo scheduled at m is executed by the PE instance located at position (i, j) at the m -th time layer. bus_x^m and bus_y^m determine the bus routing among PEs [6]. Each edge in E_{CG} denotes a resource conflict between the two bindings which cannot coexist in any independent set of CG. Section 4 details the construction of CG. The MIS of CG means the most bindings without conflict.

3.2 Problem Definition

The scheduling determines the scheduling and modulo scheduling times for each node in V_D , where the modulo scheduling time of each node indicates the time layer of the TEC when that node is operated. In Table 1, we list all the symbols used in the following texts. The scheduling can be defined as finding a scheduling $\{m(v) \mid m(v) = t(v) \% \Pi, v \in V_D\}$, such that:

- (1) $\forall (v_1, v_2) \in E_R, t(v_2) = t(v_1); \forall (v_1, v_2) \in E_W, t(v_2) = t(v_1) + 1; \forall (v_1, v_2) \in E_I, t(v_2) - t(v_1) \geq 1;$
- (2) $\forall i$ from 0 to $\Pi - 1, |\mathcal{M}_R(i)| + |\mathcal{M}_{MC}(i)| \leq M; |\mathcal{M}_W(i)| \leq N; |\mathcal{M}_{OP}(i)| + |\mathcal{M}_C(i)| \leq N \times M;$
- (3) Minimizing Π ;
- (4) On the premise of (3), minimizing $\sum_{i=0}^{\Pi-1} |\mathcal{M}_C(i)|$ and $|\mathcal{MCID}|$.

(1) and (2) respect the constraints of dependencies and modulo resources. (3) is the top concern, i.e. minimizing Π to maximize the streaming CGRA throughput. On the promise of minimizing Π , we pursue to minimize the COPs and MCIDs to ensure the optimal throughput of streaming CGRA.

The binding decides the physical resources that operate the nodes in V_D at the corresponding time layers of the TEC without resource conflicts. The binding can be defined as finding a binding set $B = \{b_1, b_2, \dots, b_k\} \subset V_{CG}$ of the conflict graph CG , such that:

- (1) $\forall b_i, b_j \in B$, then $(b_i, b_j) \notin E_{CG}, (b_j, b_i) \notin E_{CG};$
- (2) $|B| = |V_D|$

Since any edge in E_{CG} denotes a resource conflict between its two bindings, (1) and (2) guarantee a valid mapping, i.e. all the nodes in V_D are bound with the resources on the streaming CGRA without resource conflict.

4 SPARSEMAP ALGORITHM

We propose SparseMap, a mapping algorithm for sparse CNNs onto streaming CGRA, which incorporates an efficient I/O data management with operations scheduling and binding, thereby ensuring optimal throughput for streaming CGRA.

SparseMap contains four phases shown in Fig. 2. ① The scheduling phase achieves the s-DFG's scheduling with reduced COPs and MCIDs by applying AIBA, Mul-CI and RID-AT techniques. To reduce the mapping passes, ② we pre-allocate routing resources for the internal dependencies. ③ We then complete the operations binding and the I/O data and internal data routing by solving the MIS on a conflict graph. Finally, ④ SparseMap handles the incomplete mapping if it occurs.

Our previous work BusMap[6] utilized the buses to route the internal data among PEs, and achieved reduced GRF access and inserted operations. BusMap focused on accelerating the applications on common CGRAs, but neglected the impact of I/O data management on the throughput of CGRA. In this paper, we implement an efficient I/O data management in ① and ③, and applies the mechanisms described in BusMap for phases ② and ④.

4.1 Scheduling with Reduced COPs and MCIDs

❶ **Algorithm overview.** We propose a scheduling approach in Algorithm 1 that consists of three main procedures. (1) To reduce the COPs and MCIDs, lines 4-28 complete the scheduling of input readings and its fanout multiplications while employing the AIBA and Mul-CI techniques. (2) Line 30 applies the RID-AT technique for each kernel to further reduce the MCIDs. (3) Line 31 finishes the scheduling of the output writings.

To minimize Π , we start from the minimum Π (MII) = $\max(\lceil \frac{|V_{OP}|}{N \times M} \rceil, \lceil \frac{|V_R|}{M} \rceil, \lceil \frac{|V_W|}{N} \rceil)$ as lines 1 shows. Lines 4-28 iteratively allocate input buses for each input reading $r \in V_R$ and schedule its fan-out multiplications $fanout(r)$. In line 10, the input reading r highly associated with scheduled input reading set is chosen and allocated with an input bus. For the r with fanouts exceeding the

Algorithm 1 Scheduling with Reduced COPs & MCIDs

Input: s-DFG $D(V_D, E_D)$, Streaming CGRA C
Output: Scheduled s-DFG $D'(V'_D, E'_D)$, Π

- 1: $MII \leftarrow \text{CalculateMII}(D, C)$; $\Pi \leftarrow MII$; Scheduling time $t \leftarrow 0$;
- 2: Modulo resource tables $T_{PE}[] \leftarrow 0$; $T_I[] \leftarrow 0$; $T_O[] \leftarrow 0$;
- 3: Unscheduled input readings $U_R \leftarrow V_R$;
- 4: **while** $U_R \neq \emptyset$ **do**
- 5: Modulo scheduling time $m \leftarrow t \% \Pi$;
- 6: **if** $T_I[m] + 1 > N$ **then**
- 7: $t \leftarrow t + 1$;
- 8: **continue**;
- 9: **end if**
- 10: $r \leftarrow \text{AIBA}(V_R, U_R, t)$; $T_I[m]++$; $r.\text{assign}(t, m)$; $U_R \leftarrow U_R - \{r\}$;
- 11: **if** $|\text{fanout}(r)| + T_{PE}[m] \leq N \times M$ **then**
- 12: **if** $|\text{fanout}(r)| \leq N$ **then**
- 13: $T_{PE}[m] \leftarrow T_{PE}[m] + |\text{fanout}(r)|$;
- 14: $\text{fanout}(r).\text{assign}(t, m)$;
- 15: **continue**;
- 16: **end if**
- 17: **if** $\text{Mul-CI}(\text{fanout}(r), T_{PE}, T_I, t, m) = \text{true}$ **then**
- 18: **continue**;
- 19: **end if**
- 20: **if** $\text{SchedwithCaching}(\text{fanout}(r), T_{PE}, t, m) = \text{true}$ **then**
- 21: **continue**;
- 22: **end if**
- 23: $\Pi \leftarrow \Pi + 1$; **goto** 2;
- 24: **else if** $\text{SchedwithCaching}(\text{fanout}(r), T_{PE}, t, m) = \text{true}$ **then**
- 25: **continue**;
- 26: **end if**
- 27: $\Pi \leftarrow \Pi + 1$; **goto** 2;
- 28: **end while**
- 29: $\text{SchedRemainMulti}()$;
- 30: $\text{RID-AT}(D, C, T_{PE}, \Pi)$;
- 31: $D' \leftarrow \text{SchedWriting}(D, C, T_{PE}, T_O, \Pi)$;
- 32: **return** D', Π ;

available modulo PEs, $\text{fanout}(r)$ would be scheduled with a caching operation in line 24. If the modulo PEs are sufficient and $|\text{fanout}(r)|$ is less than the amount of fan-out PEs on an input bus, $\text{fanout}(r)$ would be scheduled at t directly. Otherwise, in line 17, we allocate more input buses for r . Concretely, we insert a new input reading node r' into the s-DFG, and establish the input dependencies between r' and the fanout multiplications of r as Fig. 4(c) show. r' and $\text{fanout}(r)$ would be schedule at t . The creation of r' and the establishment of input dependencies above model the multi-casting of r . If the Mul-CI loses efficacy, we try to schedule $\text{fanout}(r)$ with a caching operation (line 20). The modulo resource tables T_{PE} and T_I are updated along with the scheduling above. The s-DFG would be rescheduled under increased Π if the scheduling for $\text{fanout}(r)$ is failed. After all input readings being scheduled, we then schedule the remained multiplications in line 29.

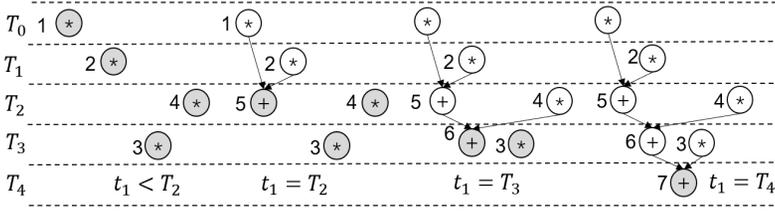


Fig. 6. Snapshots of RID-AT. Grey nodes are unaccumulated.

Finally, we reconstruct internal dependencies for the adder tree in each kernel and schedule each output writing in lines 30-31.

② **RID-AT.** To further reduce the MCIDs, the internal dependencies within the adder tree for each kernel are greedily reconstructed according to the multiplications' scheduling. Assume that t_0 is earliest scheduling time among the multiplications. As soon as two unaccumulated operations (multiplications or additions) have been scheduled before $t_1 = t_0 + 1$ and modulo PEs are available at t_1 , we schedule an addition v_a at t_1 , and then construct the internal dependencies between these two operations and v_a . Then these two operations and v_a are set as accumulated and unaccumulated statuses respectively. Otherwise, $t_0 = t_0 + 1$, repeat the process above until only one unaccumulated addition is left. Fig. 6 presents the snapshots of RID-AT for the kernel in Fig. 5.

③ **Output writing scheduling.** To correctly route the output data, the scheduling distance between the output writing and its producer must be 1. Assume that the last addition v_a in a kernel is scheduled at t_2 . An output writing w would be scheduled at $t_3 = t_2 + 1$ if the modulo output buses T_O at the modulo time $t_3 \% \Pi$ are available; Otherwise, a COP v_c is required for v_a . The v_c , as the new producer of w , would be attempted to schedule at every time slot after t_3 until the scheduling constraint for the output writing above is met.

4.2 Binding with Conflict graph

Given the scheduled s-DFG and TEC, a conflict graph is constructed to represent the binding problem, and the legal operation binding, and I/O data and internal data routing are obtained by solving the MIS on the graph. The conflict graph construction contains:

① **Vertices generation.** (1) I/O reading/writing binding: $\forall r \in V_R$ ($w \in V_W$) modulo scheduled at m , all the input (output) buses on m -th time layer of TEC are feasible. Hence, the tuples in V_{CG} can be represented as $\{(r^m, ibus_i^m) \mid \forall r \in V_R, i = 1, 2, \dots, M\} \cup \{(w^m, obus_j^m) \mid \forall w \in V_W, j = 1, 2, \dots, N\}$. (2) Operation binding: The operation binding can be expressed as quadruple $(pe_{i,j}^m, op^m, bus_x^m, bus_y^m)$ which can be referred to BusMap.

② **Edges Creation.** $\forall v_1, v_2 \in V_{CG}$, an undirected edge is created between v_1 and v_2 if resource conflicts occur. Assume that $(z, xbus)$ represents the binding of input reading ($z = r, xbus = ibus$) or output writing ($z = w, xbus = obus$). $\forall v_1, v_2$ and $v_3 \in V_{CG}$, assume that $v_1 = (z_1^{m_1}, xbus_p^{m_1})$, $v_2 = (z_2^{m_2}, xbus_q^{m_2})$ and $v_3 = (pe_{i,j}^{m_3}, op^{m_3}, bus_x^{m_3}, bus_y^{m_3})$. We apply the rules proposed in BusMap for the edge creations between any two operation bindings (quadruples). The rules related to I/O reading/writing bindings (tuples) are listed as follows:

- R1. For v_1 and v_2 , (1) $z_1 = z_2$; (2) $m_1 = m_2, xbus_p = xbus_q$. If any of (1) or (2) satisfies, the conflict occurs.
- R2. For v_1 and v_3 , (1) $(z_1, op) \in E_R, p \neq j$ or $(op, z_1) \in E_W, q \neq i$; (2) $m_1 = m_3, z_1 \in V_R, p = j, bus_y^{m_3} \neq \infty$ or $z_1 \in V_W, q = i, bus_x^{m_3} \neq \infty$. If any of (1) or (2) satisfies, the conflict occurs.

Table 2. The features of blocks

blocks	sparsity	C_nK_m	$ V_{OP} $	$ V_R $	$ V_W $	N_{FG4}
block1	0.33	C_4K_6	26	4	6	3
block2	0.33	C_4K_6	26	4	6	2
block3	0.42	C_6K_6	36	6	6	3
block4	0.21	C_4K_6	32	4	6	3
block5	0.48	C_8K_8	58	8	8	3
block6	0.62	C_8K_8	40	8	8	2
block7	0.48	C_8K_8	58	8	8	4

R1 respects the exclusiveness: any I/O reading/writing allocated to more than one I/O buses or any I/O bus occupied by more than one I/O readings/writings at the same time is forbidden. R2 ensures the correction of I/O data routing, i.e., the I/O reading/writing must be bus-connected to the PEs consuming/producing the I/O data, and these buses are not allowed for bus routing.

We apply SBTS [24] to solve the MIS on CG to get the most bindings without conflict. If $|MIS| = |V_D|$, a valid mapping is found. Otherwise, incomplete mapping happens and is then handled by the incomplete mapping processing proposed in BusMap.

5 EVALUATION

5.1 Experiment Setup

We randomly generate 5 sparse blocks wherein each weight in the blocks is set as zero value with a probability of 0.4. Additionally, we choose 2 sparse blocks from sparse models of VGGNet [18] and AlexNet[19], denoted as “block6” and “block7”. Table 2 lists the features of the blocks. C_nK_m denotes the sparse block computes n channels from m kernels. N_{FG4} is the amount of input readings with fanout size greater than 4.

We evaluate SparseMap against BusMap [6] and Zhao et al. [12] on a streaming CGRA configured as 4×4 PEA, LRF with capacity of 8 and GRF with capacity of 8.

5.2 Mapping Result Comparison

To clearly reveal the impacts of COPs and MCIDs on the throughput of the streaming CGRA, in Table 3, we list the initiation intervals II_0 , the number of COPs $|C|$, and the number of MCIDs $|M|$ of the first mapping attempt as well as the finally achieved initiation intervals II and speedups S for all the blocks. Since the works [6] [12] adopted the same scheduling heuristic[23], both works achieve the same mapping results. Due to no awareness of the irregular input data demands in heuristic [23], excessive COPs and MCIDs occur for [6] [12], leading to no success in the first mapping attempt for “block1”, “block5” and “block7”. They then try to map these blocks under increased II , however, the high routing pressures caused by the tremendous MCIDs hinder the successful mappings for “block5” and “block7”. With efficient I/O data management as well as the reconstruction of internal dependencies within adder trees, SparseMap not only reduces 92.5% COPs and 46.0% MCIDs, but also achieves the MIIs for all the blocks in the first mapping attempts. Additionally, compared with accelerating corresponding dense blocks, SparseMap realizes the speedups ranging from 1.5 to 2.67.

5.3 Ablation Study

To figure out the impacts of AIBA, Mul-CI and RID-AT techniques on the COPs and MCIDs, we conduct an experiment in which these techniques are gradually introduced into SparseMap. From Table 4, we observe that the Mul-CI technique plays an important role to reduce the COPs and

Table 3. Mapping result comparison

Tech.		Baselines[6][12]						SparseMap						
blocks	MII	First Mapping Attempt				Final		First Mapping Attempt				Final		
		II_0	$ C $	$ M $	Success?	II	S	II_0	$ C $	$ M $	Success?	II	S	
block1	2	2	3	5	N	3	1	2	0	2	Y	2	1.5	
block2	2	2	4	2	Y	2	1.5	2	0	1	Y	2	1.5	
block3	3	3	5	11	Y	3	1.67	3	1	4	Y	3	1.67	
block4	2	3	4	5	Y	3	1	2	0	3	Y	2	1.5	
block5	4	5	9	16	N	Failed		4	1	8	Y	4	2	
block6	3	3	7	8	Y	3	2.67	3	0	5	Y	3	2.67	
block7	4	5	8	16	N	Failed		4	2	11	Y	4	2	
Total	-		40	63	-				3	34	-			
									↓ 92.5%	↓ 46.0%				

Table 4. The impacts of different combinations on COPs and MCIDs

Combinations	AIBA				AIBA + Mul-CI				AIBA + Mul-CI + RID-AT (SparseMap)			
	II_0	$ C $	$ M $	II	II_0	$ C $	$ M $	II	II_0	$ C $	$ M $	II
block1	2	3	10	3	2	0	3	2	2	0	2	2
block2	2	2	12	3	2	0	3	2	2	0	1	2
block3	3	3	11	3	3	0	7	3	3	1	4	3
block4	3	3	11	3	3	0	5	3	2	0	3	2
block5	5	3	23	Failed	4	0	13	4	4	1	8	4
block6	3	2	14	3	3	0	11	3	3	0	5	3
block7	5	5	25	Failed	4	2	24	Failed	4	2	11	4

MCIDs. On the one hand, for the input readings with highly fan-out multiplications, the Mul-CI technique allocates more than one input buses for the input readings, making more multiplications obtain the input data from the input buses directly. The Mul-CI enables more multiplications to be scheduled at the same time as the input readings, thus avoiding the COPs. On the other hand, the more multiplications scheduled together guarantee the effectiveness of the AIBA technique, thereby reducing the MCIDs. After introducing the RID-AT technique, the MCIDs are further reduced for all the blocks, but with slightly increased COPs for “block3” and “block5”.

6 CONCLUSION

To address the issue of excessive COPs and MCIDs resulting from the irregular input data demands inside sparse CNNs, we propose SparseMap, a mapping algorithm for sparse CNNs on streaming CGRAs. SparseMap employs an efficient I/O data management and operation scheduling & binding to ensure optimal throughput of streaming CGRAs. Compared to previous works, SparseMap achieves fewer COPs and MCIDs while having the same or even better throughput.

ACKNOWLEDGMENTS

The authors would like to thank Information Science Laboratory Center of USTC for the hardware & software services.

REFERENCES

- [1] Nowatzki T, Gangadhar V, Ardalani N, et al. Stream-dataflow acceleration[C]//Proceedings of the 44th Annual International Symposium on Computer Architecture. 2017: 416-429.
- [2] Liu L, Li Z, Yang C, et al. HReA: An energy-efficient embedded dynamically reconfigurable fabric for 13-dwarfs processing[J]. *IEEE Transactions on Circuits and Systems II: Express Briefs*, 2017, 65(3): 381-385.
- [3] Yongjoo Kim, Jongeun Lee, Aviral Shrivastava, and Yunheung Paek. 2011. Memory access optimization in compilation for coarse-grained reconfigurable architectures. *ACM Trans. Des. Autom. Electron. Syst.* 16, 4, Article 42 (October 2011), 27 pages. <https://doi.org/10.1145/2003695.2003702>
- [4] Jonghee W. Yoon, Jongeun Lee, Sanghyun Park, Yongjoo Kim, Jinyong Lee, Yunheung Paek, and Doosan Cho. 2013. Architecture customization of on-chip reconfigurable accelerators. *ACM Trans. Des. Autom. Electron. Syst.* 18, 4, Article 52 (October 2013), 22 pages. <https://doi.org/10.1145/2493384>
- [5] Hamzeh M, Shrivastava A, Vrudhula S. REGIMap: Register-aware application mapping on coarse-grained reconfigurable architectures (CGRAs)[C]*Proceedings of the 50th Annual Design Automation Conference*. 2013: 1-10.
- [6] X. Ni et al. BusMap: Application Mapping with Bus Routing for Coarse-Grained Reconfigurable Array, in *IEEE Transactions on Circuits and Systems II: Express Briefs*, doi: 10.1109/TCSII.2023.3253686.
- [7] Kou M, Gu J, Wei S, et al. TAEM: fast transfer-aware effective loop mapping for heterogeneous resources on CGRA[C]. *2020 57th ACM/IEEE Design Automation Conference (DAC)*. IEEE, 2020: 1-6.
- [8] Kou M, Zeng J, Han B, et al. GEML: GNN-based efficient mapping method for large loop applications on CGRA[C]. *Proceedings of the 59th ACM/IEEE Design Automation Conference*. 2022: 337-342.
- [9] Yin S, Yao X, Liu D, et al. Memory-aware loop mapping on coarse-grained reconfigurable architectures[J]. *IEEE Transactions on Very Large Scale Integration (VLSI) Systems*, 2015, 24(5): 1895-1908.
- [10] Dave S, Balasubramanian M, Shrivastava A. RAMP: Resource-aware mapping for CGRAs[C]. *Proceedings of the 55th Annual Design Automation Conference*. 2018: 1-6.
- [11] Hamzeh M, Shrivastava A, Vrudhula S. EPIMap: Using epimorphism to map applications on CGRAs[C]. *Proceedings of the 49th Annual Design Automation Conference*. 2012: 1284-1291.
- [12] Zhao Z, Sheng W, Wang Q, et al. Towards higher performance and robust compilation for cgra modulo scheduling[J]. *IEEE Transactions on Parallel and Distributed Systems*, 2020, 31(9): 2201-2219.
- [13] Friedman S, Carroll A, Van Essen B, et al. SPR: an architecture-adaptive CGRA mapping tool[C]*Proceedings of the ACM/SIGDA international symposium on Field programmable gate arrays*. 2009: 191-200.
- [14] H. Park, K. Fan, S. A. Mahlke, T. Oh, H. Kim, and H.-S. Kim, "Edge-centric modulo scheduling for coarse-grained reconfigurable architectures," in *Proc. 17th Int. Conf. Parallel Archit. Compilation Techn.*, 2008, p. 166
- [15] Wijerathne D, Li Z, Bandara T K, et al. PANORAMA: divide-and-conquer approach for mapping complex loop kernels on CGRA[C]. *Proceedings of the 59th ACM/IEEE Design Automation Conference*. 2022: 127-132.
- [16] Kong X, Huang Y, Zhu J, et al. Mapzero: Mapping for coarse-grained reconfigurable architectures with reinforcement learning and monte-carlo tree search[C]//Proceedings of the 50th Annual International Symposium on Computer Architecture. 2023: 1-14.
- [17] Liu D, Xia Y, Shang J, et al. E2EMap: End-to-End Reinforcement Learning for CGRA Compilation via Reverse Mapping[C]//2024 IEEE International Symposium on High-Performance Computer Architecture (HPCA). IEEE, 2024: 46-60.
- [18] Simonyan K, Zisserman A. Very deep convolutional networks for large-scale image recognition[J]. *arXiv preprint arXiv:1409.1556*, 2014.
- [19] Krizhevsky A, Sutskever I, Hinton G E. Imagenet classification with deep convolutional neural networks[J]. *Advances in neural information processing systems*, 2012, 25.
- [20] D. Amodei, D. Hernandez, G. Sastry, J. Clark, G. Brockman, and I. Sutskever, "Ai and compute," <https://openai.com/blog/ai-and-compute/>, May 2018.
- [21] Deng C, Liao S, Xie Y, et al. PermDNN: Efficient compressed DNN architecture with permuted diagonal matrices[C]//2018 51st Annual IEEE/ACM international symposium on microarchitecture (MICRO). IEEE, 2018: 189-202.
- [22] X. Zhou, Z. Du, Q. Guo, S. Liu, C. Liu, C. Wang, X. Zhou, L. Li, T. Chen, and Y. Chen, Cambricon-s: Addressing irregularity in sparse neural networks through a cooperative software/hardware approach, in *2018 51st Annual IEEE/ACM International Symposium on Microarchitecture (MICRO)*. IEEE, 2018, pp. 15–28.
- [23] Llosa J, Ayguadé E, Gonzalez A, et al. Lifetime-sensitive modulo scheduling in a production environment[J]. *IEEE Transactions on Computers*, 2001, 50(3): 234-249.
- [24] Jin Y, Hao J K. General swap-based multiple neighborhood tabu search for the maximum independent set problem[J]. *Engineering Applications of Artificial Intelligence*, 2015, 37: 20-33.

Received 20 February 2007; revised 12 March 2009; accepted 5 June 2009